Eur Biophys J (2005) 34: 208–216
DOI 10.1007/s00249-004-0442-z

ARTICLE

Ben Corry · Shin-Ho Chung

Influence of protein flexibility on the electrostatic energy landscape in gramicidin A

Received: 19 July 2004 / Revised: 22 September 2004 / Accepted: 28 September 2004 / Published online: 5 November 2004

Abstract We describe an electrostatic model of the gramicidin A channel that allows protein atoms to move in response to the presence of a permeating ion. To do this, molecular dynamics simulations are carried out with a permeating ion at various positions within the channel. Then an ensemble of atomic coordinates taken from the simulations are used to construct energy profiles using macroscopic electrostatic calculations. The energy profiles constructed are compared to experimentally-determined conductance data by inserting them into Brownian dynamics simulations. We find that the energy landscape seen by a permeating ion changes significantly when we allow the protein atoms to move rather than using a rigid protein structure. However, the model developed cannot satisfactorily reproduce all of the experimental data. Thus, even when protein atoms are allowed to move, the dielectric model used in our electrostatic calculations breaks down when modeling the gramicidin channel.

Keywords Ion channels · Molecular dynamics · Gramicidin A · Electrostatics · Brownian dynamics · Conductance · Ion permeation · Simulation · Protein motion

Introduction

The transport of ions through protein channels is a fundamental biological process and has recently been the focus of much theoretical investigation. The first channel for which we knew the detailed atomic structure was the antibiotic polypeptide gramicidin A (GA). It is a β-helical head-to-head dimer that forms a narrow single file channel (Urry 1971). Recently, high resolution structures have been determined using solution NMR (Arseniev et al. 1985; Townsley et al. 2001) and solid-state NMR studies (Ketchem et al. 1993, 1997; Separovic 1999). In the absence of structural information for biological ion channels, the GA channel was for a long time the main focus of theoretical investigations (Partenskii and Jordan 1992; Roux and Karplus 1994). Although the focus has now shifted to the recently crystallized potassium (Doyle et al. 1998), mechanosensitive (Chang et al. 1998) and chloride channels (Dutzler et al. 2002), GA remains a useful test case. The GA protein is small, consisting of only 30 amino acid residues. Although this small size makes the channel easier to model in some ways, it also leads to some great difficulties. The channel is very narrow, having a radius of only 2 Å for most of its length, thus creating a single file channel in whose narrow confines the bulk diffusion properties of ions and water become skewed. Thus, this channel provides a stringent test case for permeation theories, and has proved extremely difficult to model accurately.

Ideally, models of ion channels will relate the atomic details of the channel to experimentally-determinable quantities such as their conductance. Unfortunately, achieving this goal is a not straightforward task. Full atomistic simulations, such as molecular dynamics simulations (MD), are very time consuming. These studies provide valuable information on the selectivity mechanism and the energetics of ion permeation in the channel, but currently cannot be run for long enough to estimate the channel conductance, or even to explore the dynamics of a single conduction event in any biological channels. One of the main uses of atomistic simulations in understanding the conductance properties of channels has been in determining the free energy landscape encountered by permeating ions. Thus, although the

B. Corry (✉)
Chemistry, School of Biomedical and Chemical Sciences,
The University of Western Australia Crawley,
WA, 6009, Australia
E-mail: ben@theochem.uwa.edu.au

S.-H. Chung
Department of Theoretical Physics,
Research School of Physical Sciences,
The Australian National University,
Canberra, ACT, 0200, Australia

current passing through a channel cannot be calculated directly, the forces acting on an ion at various positions in the channel can be determined, and these may be used in lower level theories to find the channel conductance. One problem with such an approach, however, has made itself clear in studies of the gramicidin A channel. Two recent studies of the potential of mean force in this channel from molecular dynamics simulations have found a very large energy barrier in the center of the channel of either 25, 17 or 11 kT in height (Allen et al. 2003a, 2004). Although a plausible current value was determined from the last profile using the Nernst–Planck equation, when any of these potential profiles are placed into the more detailed Brownian dynamics simulations we find that no ions cross the channel and so the experimental conductance is not reproduced.

Permeation models of lower resolution, such as Brownian dynamics (BD) (Cooper et al. 1985; Kuyucak et al. 2001) and Poisson–Nernst–Planck equations (Levitt 1986; Eisenberg 1999) have long been considered in the literature. The latter approach has recently been shown to be invalid in a narrow pore environment because it neglects the self-energy of ions (Corry et al. 2000). Attempts to explicitly add such self energy to these models have led to some improvements in very narrow channels (Mamonov et al. 2003; Corry et al. 2003; Koumanov et al. 2003) but such theories are still not reliable at all channel radii (Corry et al. 2003). The Poisson–Nernst–Planck models are designed for use in systems containing a large number of ions, which is obviously not satisfied in all ion channels, and they find describing ion–ion interactions in multi-ion channels difficult. For this reason we believe that BD simulations remain the most reliable computationally tractable tool for calculating a channel's conductance from its structure.

A common feature of these simplified models is that they usually treat the channel protein as a rigid dielectric environment. Although the partial charges of all of the protein atoms can be included, they do not move in response to a permeating ion. Recent rigid dielectric models of the GA channel have not had complete success. Electrostatic calculations utilizing the high-resolution NMR structures could either predict the correct current–voltage behavior but not binding sites and saturation at high concentration, or none of these depending on the choice of dielectric constants (Edwards et al. 2002). We are left to consider whether the model failed because it did not allow atomic motions within the protein, or because it is not possible to give an accurate dielectric representation of a single file of water molecules. The use of a rigid protein structure in simplified theories has been questioned many times in the literature (Elber et al. 1995; Im and Roux 2002; Nadler et al. 2003; Feig and Brooks 2004) and determining its validity is important if these models are going to continue to be used.

In an attempt to answer this question, we here utilize a composite MD, electrostatic and BD approach that can incorporate the motions of atoms within the channel protein into a dielectric model. MD simulations are carried out with a permeating ion in various positions in the channel to sample possible protein motions. Then, an ensemble of protein configurations are taken from the MD simulations, and the energy of, and forces on, the permeating ion are calculated from these using Poisson's equation. The macroscopic conductance properties of the channel are then determined by using these forces in BD.

In this paper, we first describe the composite model, use it to calculate the energy landscape encountered by a permeating ion, and finally calculate the conductance properties of the channel to compare with experimental measurements.

Methods

Composite MD and electrostatic calculations

Molecular dynamics simulations of the GA dimer embedded in a bilayer consisting of 96 dimyristoylphosphatidylcholine (DMPC) molecules and 3,209 water molecules were carried out in an electroneutral solution of 150 mM KCl with GROMACS 3.0 (Lindhal 2001; Berendsen 1995) utilizing the CHARMM PARAM 27 (Mackerrel et al. 1998) force field. A constant pressure of 1 atm was applied in the z-direction and a surface tension of 46 dyn/cm in the xy plane. As the simulation methods are given in Allen et al. (2003a), we do not describe them here in detail. The simulations use as a starting structure one monomer with the coordinates given by Ketchem et al. (1997) and one using those of Koeppe et al. (1994). Although a recent study by Allen et al. (2003b) suggests that the structure of Townsley et al. (2001) would provide a better starting point for our simulations, Allen et al. (2003b) find that the structures become almost indistinguishable during dynamic simulation. The initial structure is equilibrated over 78 ps including steepest decent minimization, heating, temperature coupling and surface tension coupling. These simulations were used to determine a PMF for a permeating ion, and as such a permeating ion was constrained in the neighborhood of many positions within the channel using a biasing potential to enable umbrella sampling. The ion was moved through the channel in 0.5 Å steps, and at each position the system was equilibrated for 10–20 ps followed by a further 50–80 ps of simulation. To utilize the results of the MD simulations in electrostatic calculations, 100 snapshots of the protein structure were taken at regular intervals during the simulation for each position of the permeating ion. At the end of the MD simulation we have saved a large number of protein atom coordinates, representing 100 different conformations of the protein for each position of the ion inside the channel.

For each snapshot of atomic coordinates taken from the MD simulations, we determine the potential energy required to bring the ion to that position. To do this we solve Poisson's equation:

$$\varepsilon_0 \nabla \cdot [\varepsilon(\mathbf{r}) \nabla \phi(\mathbf{r})] = -\rho(\mathbf{r}),$$

in which $\phi(\mathbf{r})$, $\varepsilon(\mathbf{r})$ and $\rho(\mathbf{r})$ are the space-dependent electric potential, relative dielectric constant and charge density respectively, and ε_0 is the permittivity of free space. The energy values determined from the 100 snapshots at each ion position are then averaged and the entire process repeated for each ion position to obtain a complete energy profile through the channel.

Poisson's equation was solved using a finite difference method described previously (Moy et al. 2000; Edwards et al. 2002) using a grid size of 0.5 Å. Partial charges are assigned from the CHARMM PARAM 27 force field. To solve Poisson's equation, we must first determine the locations of the channel walls and ascribe dielectric constants to the various regions (see Edwards et al. (2002), for a more complete description). We assign radii to each atom following the scheme derived by Li and Nussinov (1998), and trace a boundary by moving a sphere along the edge of the pore.

In Fig. 1, we show the channel boundary calculated when there is no ion in the channel (solid line), when there is an ion at $z = -9$ Å (dashed line), and when there is an ion in the center of the channel (dotted line), averaging the 100 different configurations for each ion position. The pore forms a narrow conduit through the membrane with an average radius of only about 2 Å. No symmetry is assumed, and so the shape of the boundary is slightly different at each azimuthal angle. It can be seen that the location of the boundary changes slightly as the permeating ion moves to different positions within the channel. A small degree of deformation is visible in the region closest to the ion, with the channel typically bending slightly toward the ion. However, the changes in the shape of the dielectric boundary are small. The choice of dielectric constants is examined in more detail below.

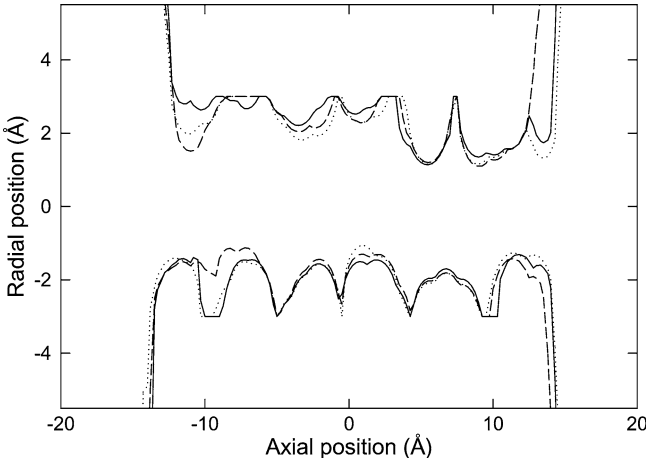

Fig. 1 Slice of the dielectric boundary in the electrostatic model of GA. The location of the channel walls are shown at one azimuthal angle with no ion in the channel (*solid lines*), an ion located at $z = -9$ Å (*dashed line*), and with an ion in the center of the channel (*dotted line*). The boundaries shown are constructed from the average atomic coordinates taken over the entirety of the corresponding MD simulation

Brownian dynamics simulations

To relate the energy profiles to the observable properties of the GA channel, we incorporate them into BD simulations. In these simulations, we place 24 K^+ ions and 24 Cl^- ions in cylindrical reservoirs of radius 30 Å at each end of the channel to mimic the extracellular and intracellular space. We adjust the height of the cylinder to 29.2 Å to bring the solution to 500 mM. We then trace the motion of these ions under the influence of electric and random forces using the Langevin equation:

$$m_i \frac{\mathrm{d}\mathbf{v}_i}{\mathrm{d}t} = -m_i \gamma_i \mathbf{v}_i + \mathbf{F}_i^{\mathrm{R}}(t) + q_i \mathbf{E}_i + \mathbf{F}_i^{\mathrm{S}}$$

Here, m_i, $\mathbf{v}_i$, $m_i\,\gamma_i$ and q_i are the mass, velocity, friction coefficient and charge on an ion with index i, while $\mathbf{F}_i^{\mathrm{R}}$, $\mathbf{E}_i$ and $\mathbf{F}_i^{\mathrm{S}}$ are the random stochastic force, electric field, and short range forces experienced by the ion, respectively. We calculate the total force acting on each and every ion in the assembly and then calculate new positions for the ions a short time later. A multiple time-step algorithm is used, where a time-step of $\Delta t = 100$ fs is employed in the reservoirs and 2 fs in the channel, where the forces change most rapidly. When simulating at different concentrations, we keep the reservoir size the same and alter the number of ions contained within it.

In most previous BD simulations the electric field is determined by solving Poisson's equation for a given rigid protein structure. In this case, however, we use the energy profiles determined above to describe the interaction of the ions with the fixed charges and protein boundary. Thus, the total force acting on an ion is the sum of the derivative of the energy profile calculated above, the direct Coulomb interaction with other ions and random and frictional terms. An additional short range $1/r^9$ potential is added to describe the overlap of an ion's electron cloud with other ions or the channel walls. Recent MD simulations have shown that a 1-D energy profile accurately represents ion motion inside the gramicidin A channel (Allen et al. 2004b). To describe the 3-D potential in the channel, the one-dimensional profile is supplemented by a harmonic constraint in the radial direction as done for the "inverse method" described in Edwards et al. (2002). Although the electrostatic energy profile calculated from the protein structures does not include Leonard–Jones interactions between the ions and the protein that are included in the MD simulations, this is unlikely to influence the BD simulations, as they use an essentially one-dimension potential calculated on the axis of the channel where the LJ forces have a negligible effect. The ion-protein interactions are also incorporated into the short-range $1/r^9$ potential. The direct Coulomb interactions between ions are calculated explicitly during the simulations in which the charge on each ion is attenuated by

the dielectric constant at the given location. The effect of any dielectric boundaries between or near the ion is incorporated in the image forces as part of the solution to Poisson's equation noted above.

The Langevin equation is solved using the algorithm of van Gunsteren and Berendsen (1982), and the techniques described by Li et al. (1998). Bulk ionic diffusion coefficients of 1.96×10^{-9} m^2 s^{-1} for K^+ and 2.03×10^{-9} m^2 s^{-1} for Cl^- ions are employed in the reservoirs and vestibules. These values are reduced to 15% of the bulk values in the pore in accordance with recent estimates from MD (Allen et al. 2000; Mamonov et al. 2003, Smith and Sansom 1999). Simulations under various conditions, each lasting 3.2–5 μs, are performed with symmetric ionic concentrations in the two reservoirs. For further technical details of the method of simulating Brownian dynamics, see Chung et al. (1998, 1999, 2002) or Corry et al. (2002).

Results

Before proceeding to discuss our findings, it is worth noting the three main pieces of experimental data to which we will compare our results. Firstly, we know the single channel current that flows through the pore, and in particular the current-voltage (I–V) curve is well-characterized. This curve is found to be linear through the origin, with a conductance that depends on the ionic concentration (Busath et al. 1998; O. S. Andersen, Department of Physiology and Biophysics, Weill Medical College of Cornell University, personal communication, 2002). Secondly, when we plot the current passing through the channel as a function of the ionic concentration, it is found that the current saturates at high concentrations (the half-saturation value at 200 mV is around $K_s\approx0.23$ M (Andersen)). This saturation is a direct result of rate limiting barriers in the channel and will not occur unless the ion has to climb substantial energy barriers to move out of the energy wells in the channel (Chung et al. 1998). Finally, from NMR studies, we expect ions to dwell for longer in binding sites near each end of the channel than elsewhere (Tian and Cross 1999).

Energy profiles

The energy landscape encountered by a permeating ion describes the forces it feels and ultimately determines the conductance of the channel. In Fig. 2a, we show the potential energy profile along the central axis of the channel calculated using Poisson's equation. We assign dielectric constants of 80 and 2 to the water and protein. When we use the NMR structure of Ketchem et al. (1997) (accession code 1MAG), we find that there are two small energy wells located near each end of the channel, separated by a low barrier (dash-dot line). As noted previously (Edwards et al. 2002), this profile is unable to reproduce or explain the three pieces of experimental data available on GA. Although it can reproduce the current–voltage curve (with an appropriate choice of diffusion coefficient), the energy wells are too shallow to show binding sites or result in saturation of currents at high concentrations.

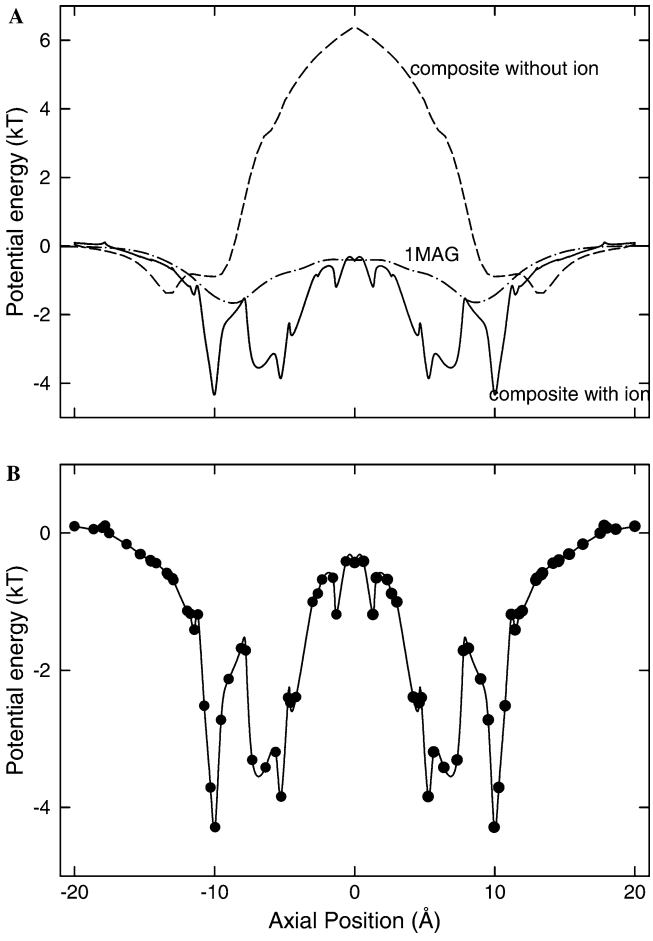

Fig. 2 The potential energy profile along the axis of the channel calculated from Poisson's equation with different protein structures. **a** The profile found using the rigid NMR coordinates of Ketchem et al. (1997) (1MAG) (*dash-dot line*) is compared to models in which an ensemble of protein atom coordinates are taken from MD simulations without an ion in the channel (*dashed line*) and with a permeating ion at each point along the profile (*solid line*). The latter profile is also shown in **b** in more detail. Dielectric constants of 80 for the bulk water and channel and 2 for the protein are used in all cases

The GA atom coordinates change slightly when we allow the structure of the channel to relax in the MD simulations with no permeating ion in the channel. The dashed line in Fig. 2a indicates the potential energy profile determined by taking an average of 100 profiles made using 100 different randomly chosen snapshots of the MD simulation without an ion in the channel. This profile still contains shallow energy wells at each end, but it now has a much larger barrier in the center of the channel. The difference between this profile and that obtained from the original NMR structure indicates that the NMR structure may not be in an appropriate en-

ergy-minimized state. Indeed, this profile is more similar to that determined from the NMR structure of Arseniev et al. (1985) than that of Ketchem et al. (1997). We cannot expect this profile to reproduce the experimental data, as the energy wells are again too shallow to create binding sites. Nor can we expect current saturation at high concentration, as the time taken for an ion to cross the central barrier is likely to remain dependent on the concentration of ions in the reservoir in this profile.

However, when we allow the permeating ion to influence the structure of the GA protein, the energy profile begins to look more plausible. The solid lines in Fig. 2a indicate the profile obtained with the combined MD–electrostatic approach in which the protein atoms can move in response to the resident ion at each position. This profile is reproduced in more detail in Fig. 2b. For each ion position used to create the profile, the energy is calculated using 100 sets of atomic coordinates obtained from MD with the ion held in the neighborhood of that position. The adjustment of the protein atoms in the presence of the permeating ion significantly lowers its potential energy. Although the profile is quite jagged, four energy wells of depth around 4 kT are clearly visible, separated by an energy barrier of a similar magnitude. To test whether this profile can reproduce the experimental data, we insert it into BD simulations as described below.

An important consideration when creating these energy profiles is the choice of dielectric constants. The value we should assign to the bulk water either side of the channel is well determined to be 80. The value we should assign to the protein is also fairly clear. As our current methodology allows the protein atoms to move in response to any electric fields (such as those created by the permeating ion), any molecular polarizability is being included explicitly. Typically, a dielectric constant of around 2 is taken to represent the electronic polarizability of a material with no molecular dipoles. Values higher than this represent the presence of molecular dipoles that can orient to any electric fields. As we are including molecular motions explicitly in the MD simulations, we should not include any molecular dipoles in our electrostatic calculations. Thus, the protein should be assigned a value of approximately 2. Using values higher than this, as has been done in a similar approach elsewhere (Mamonov et al. 2003), only acts to double count the molecular polarizability of the protein.

The dielectric constant in the channel is less well-defined. It is likely that in the confines of the narrow GA channel, water molecules will be less able to orient to the electric field than in bulk solution. We can therefore expect the value to be somewhat lower than 80. To examine this possibility, in Fig. 3 we show the energy profile obtained with a dielectric constant of 60 inside the channel (dashed lines) in comparison to that found with a value of 80. When we use a dielectric constant of 60 in the channel, we still use a value of 80 in the bulk solution, and vary the dielectric constant smoothly between these values at the mouth of the channel (between

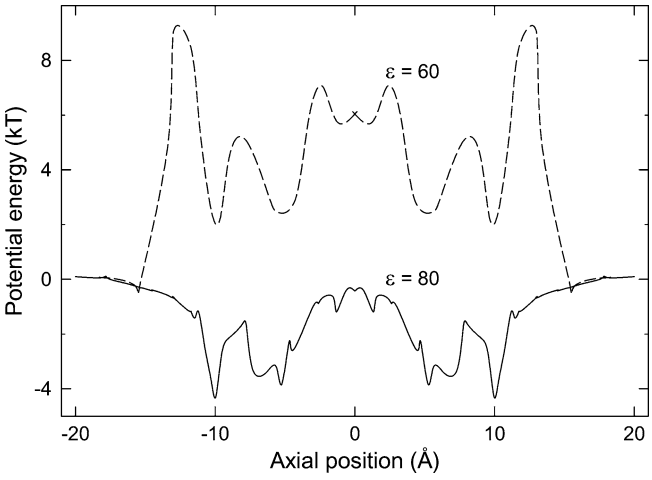

Fig. 3 The potential profile calculated using the composite MD/electrostatic model with differing dielectric constants. The dielectric constant of the protein is maintained at 2 and that of bulk water at 80, while that in the channel is set to 80 (*solid line*) or 60 (*dashed line*)

$z = 12.5$ and $z = 17.5$ Å). Using a dielectric constant of 60 amplifies the features of the energy profile, but it also introduces a new barrier at each end of the channel. The barrier is caused by the change in the dielectric self-energy of the ion as it has to move from a region of high dielectric constant into a region with a lower one. This barrier is very high, indeed it is such that it makes ion permeation almost impossible. Since the barrier height will increase as we lower the dielectric constant in the channel, we do not illustrate the results with lower values here (see Edwards et al. (2002) for an illustration of the use of low dielectric constants in the channel). Thus, the profile that is most likely to reproduce experimental data is that obtained with a dielectric value of 80 in the channel.

It is worth comparing our results to those of a similar study published previously. Mamonov et al. (2003) also incorporate protein dynamics into an electrostatic model in a similar way, albeit with a different set of partial charges and protein dielectric constant, and a simpler MD lipid model. They find a very similar profile when a dielectric constant of 80 is assigned inside the channel. Although there are some small differences, the major features—including energy wells of $\sim$ 4 kT in depth—are alike. This suggests that the broad features of the energy profile are not highly dependent on the MD system or sampling used to obtain protein coordinates.

Currents determined from Brownian dynamics

In Fig. 4, we show the current voltage curve obtained by putting the composite energy profile into BD simulations with a symmetric concentration of 500 mM KCl in the reservoirs. The simulated data (filled circles) is close to linear, and by choosing the correct diffusion coefficient it agrees well with the experimental data of

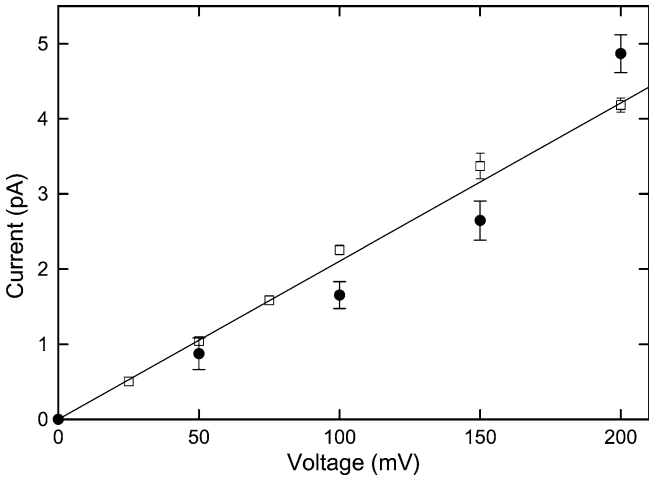

Fig. 4 Current–voltage curve of GA obtained using BD simulations with the energy profile shown in Fig. 2b. The simulated data (*filled circles*) are compared to the experimental data of Andersen obtained in diphytanoylPC lipid bilayers (private communication *open squares*). A concentration of 500 mM KCl is used in both cases

Andersen shown by the open squares. As noted previously (Edwards et al. 2002) Cl^- ions see a potential energy barrier in the channel, due to slightly more negative partial charges in the protein residing near the pore, and so do not enter.

However, despite this promising agreement between the I–V curves, the simulated data does not agree as well with experiment in regard to the other experimental data. Firstly, we show the current-concentration relationship under an applied potential of 200 mV in Fig. 5. Whereas the experimental data of Andersen (open squares) shows clear saturation, with a half maximum value of $K_s \approx 230$ mM, the simulated data shows no sign of saturation. Indeed, the simulated current increases linearly up to the highest simulated concentration of 1.5 M.

Finally, we show where ions dwell in the channel during our simulation in Fig. 6. There are two regions near each end of the channel where there is a slight increase in the probability of finding an ion, corresponding to the energy wells seen in the composite energy profile. The end bins in the histogram ($|z| > 15$) represent the entrances of the channel and are occupied at a slightly higher concentration than the bulk solution. On average, we find that in the absence of an applied field, with a 500 mM concentration in the reservoirs, the channel holds 0.57 ions including these bins or 0.35 ions excluding them. Some evidence of preferential binding is visible, although it is not as obvious as that expected from previous studies (Edwards et al. 2002). It may, however, be enough to explain the binding sites seen in NMR studies.

Discussion

In this study, we have incorporated protein dynamics into an electrostatic model of the gramicidin channel. To do this, we carried out MD simulations to sample the range of possible motions of the protein atoms encountered as an ion permeates through the channel. Electrostatic calculations were then made for an ensemble of protein structures with the ion located in a large number of positions along the channel. Thus, the electrostatic energy profile we calculate allows for protein atoms to move in response to ion translocation. The energy profile thus constructed was then inserted into a BD simulation to determine the currents that would flow through the channel.

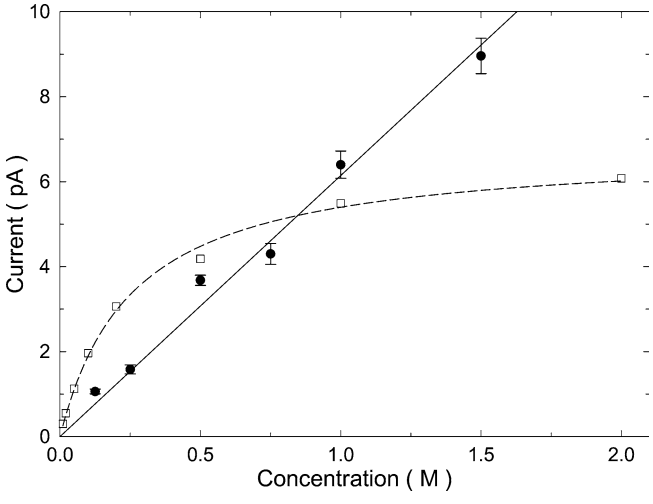

Fig. 5 Current–concentration relationship of GA obtained using BD simulations with the energy profile shown in Fig. 2B. The simulated data (*filled circles*) are compared to the experimental data of Andersen (private communication *open squares*). A potential of 200 mV is used in both cases

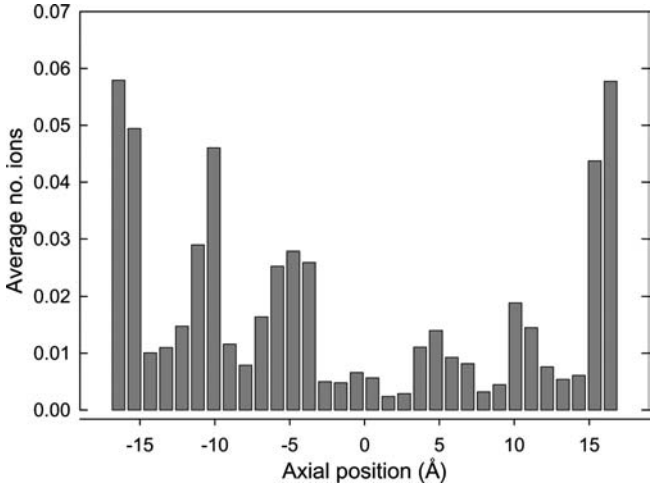

Fig. 6 Ion-dwell histogram obtained from BD simulations with the energy profile shown in Fig. 2b. The channel is divided into 32 layers and the average number of ions in each is shown for a 0.3 μ simulation with 500 mM KCl in the reservoirs and no applied potential

Our calculations yield two important conclusions. Firstly, protein motions during ion permeation do appear to significantly influence the energy landscape seen by an ion permeating through GA. A comparison of the energy profile calculated using our composite approach without an ion in the channel, and with the permeating ion, show a difference of up to 6 kT. This is remarkable when it is apparent that the location of the channel boundary does not change significantly as the ion permeates through the channel (Fig. 1). This result is in agreement with the conclusion derived by Dorman and Jordan (2004). Using the semi-microscopic method, they show that the height of the central barrier in the permeation free energy for alkaline cations moving across GA is reduced substantially when the peptide backbones are allowed to move. Our preliminary results also suggest that protein flexibility can alter the potential of mean force calculated in a molecular dynamics simulation. It appears that only a small movement of the protein atoms is required to substantially alter the energy landscape in the channel. Thus, using a rigid protein structure when modeling gramicidin A appears incorrect. Whether this conclusion also applies to other biological ion channels remains to be determined, as it is possible that the effect of the motion of protein atoms on the energy of the permeating ion is greater in GA due to its narrow radius. Inside a wider channel, or in the central chamber of the KcsA channel, such small protein motions are likely to be screened out by surrounding water molecules and have less effect.

Secondly, we find that our electrostatic model of the channel still cannot replicate all of the experimental data, even when protein motions are allowed. Although the energy profiles calculated here look more promising than when we use a rigid channel structure, they still cannot reproduce the saturation of current at large concentrations. The underlying culprit for these problems is probably the use of continuum electrostatics itself. That is to say, the use of dielectric constants, that are macroscopic averages of underlying microscopic phenomena, is probably not appropriate in the confined space within the GA channel. Ultimately, it is likely that a single file chain of water molecules in a confined space cannot be described by a (uniform) dielectric constant.

The lack of clear binding sites and saturation in current at high concentration are a consequence of the energy wells in the composite profile being too shallow. Deeper wells would hold permeating ions for longer, creating more obvious binding sites. Also, this would make it harder for ions to exit the wells, making this a more time consuming step during permeation. The time taken for ions to exit the well would not depend on concentration in the reservoirs and so deeper wells could be expected to create saturation in the current–concentration relationship. Thus, this study confirms the results seen previously (Edwards et al. 2002; Chiu and Jakobsson 1989; McGill and Schumaker 1996) in which well depths of at least 5–8 kT are required to match the experimental data.

It is worth again comparing our results with those of Mamonov et al. (2003), who place a similar energy profile into Poisson-Nernst-Planck theory (with explicit dielectric self-energy included) to determine the channel conductance. In that study, the I–V curves and binding are similar to those seen here, but saturation is apparent in the concentration-conductance curve. The reason for this disparate result lies in the different conduction models used. In our BD model, we find that as we increase the bath concentration, the concentration of K^+ ions in the channel also increases. In the earlier study, the concentration inside the channel does not increase significantly, even when the bath concentration is increased to 10 M. This may well be a spurious result, caused by the explicit inclusion of dielectric self-energy, which has often been seen elsewhere (Corry et al. 2003) to reduce channel concentrations too much.

There are obvious problems with using a dielectric description in a single file channel, and forces that the dielectric description does not capture. For example, as a permeating ion in GA has only one water molecule on each side, it is difficult for these to shield out partial charges close by in the direction perpendicular to the axis of the channel. Also, it is likely that the water molecules near to the ion will be aligned with the negative ends of their dipoles pointing toward a permeating cation. As an ion enters the channel, such a line of water molecules may have an attractive effect, pulling the ion into the channel. Reorienting any one of the water molecules would be difficult if they are in a well-aligned sequence.

When considering the appropriateness of the scheme used in this study for incorporating protein flexibility into the electrostatic model, it is important to consider the timescales of the various processes that influence the electrostatic potential. As an ion permeates through the channel, the protein will alter its conformation slightly in response to the field created by the passing ion. The average change in conformation induced by the passing ion, however, remains for as long as the ion is present. Thus, when an ion resides in any form of energy well or binding site, the protein conformation it induces is relatively long-lived. When we solve Poisson's equation for each protein configuration we allow some degree of relaxation in the protein and water environment that is implicit in the use of dielectric constants. By assigning a dielectric constant of 2 to the protein we allow for electronic polarization in the atoms. This, however, takes place over time-spans much shorter than the lifetime of the induced protein conformation. Assigning a dielectric constant of 80 to the aqueous environment also allows for water molecules to re-orientate to the field created by the changing protein conformation. If the protein undergoes only small conformational changes, the reorientation of water molecules induced by this will be almost negligible compared to those induced by the presence of a permeating ion. Furthermore, if the average conformational change induced by the passing ion is long-lived, allowing nearby water molecules to

readjust would seem appropriate. Indeed, the readjustment of water molecules takes place over a timescale of tens of picoseconds. This is much shorter than the diffusion time of the permeating ion. Thus, the timescale of the implicit relaxation of the environment captured in the dielectric constants is shorter than the lifetime of the change in protein conformation induced by the permeating ion. From this point of view, the technique of solving Poisson's equation for each protein conformation is an appropriate way of determining the electrostatic energy landscape encountered by the ion in the channel.

It is possible to incorporate the motion of protein atoms into BD simulations without using macroscopic electrostatics and dielectric constants. One way is to calculate the energy profile experienced by a permeating ion directly from MD and insert this into BD simulations to determine channel conductance. This scheme would explicitly incorporate the effects of ion dehydration as it enters the channel, as well as entropic effects, and would obviate the need for assigning dielectric constants within the channel. Unfortunately, however, in the case of gramicidin A, such an approach is not currently feasible. Recent calculations of the potential of the mean force determined from MD simulations all contain a large central barrier that would prevent ion permeation (Jordan 1990; Roux and Karplus 1993; Allen et al. 2003a). The origins of this problem, which may lie in the parameterization of the MD simulations or their lack of electronic polarizability, need to be determined and fixed before we can model GA this way. However, this approach has recently been used for studying the KcsA potassium channel by Bernéche and Roux (2003) in which a two-dimensional potential of mean force for the selectivity filter of the channel is incorporated into a BD simulation of ions in this region. This approach looks promising, and it will be interesting to see the results of incorporating a potential of mean force calculated along the entire length of the KcsA protein into a BD simulation of the entire channel and surrounding reservoirs. For the time being, at least, it appears that neither atomistic simulations nor macroscopic electrostatic models can be reliably used to predict the current passing through the gramicidin channel.

Acknowledgements The authors wish to thank Dr. Turgut Bastug for supplying protein coordinates from his MD calculations. This work was supported by grants from the Australian Research Council, the Australian Partnership of Advanced Computing and the National Health and Medical Research Council of Australia. The calculations upon which this work is based were carried out using the Compaq AlphaServer SC of the Australian Partnership for Advanced Computing.

References

Allen TW, Kuyucak S, Chung SH (2000) Molecular dynamics estimates of ion diffusion in model hydrophobic and KcsA potassium channels. Biophys Chem 86:1–14

Allen TW, Bastug T, Kuyucak S, Chung SH (2003a) Gramicidin A channel as a test ground for molecular dynamics force fields. Biophys J 84:2159–2168

Allen TW, Andersen OS, Roux B (2003b) Structure of gramicidin A in a lipid bilayer environment determined using molecular dynamics simulations and solid-state NMR data. J Am Chem Soc 125:9868–9877

Allen TW, Andersen OS, Roux B (2004) Energetics of ion conduction through the gramicidin channel. Proc Natl Acad Sci USA 101:117–122

Arseniev AS, Barsukov IL, Bystrov VF, Lomize AL, Ovchinnikov YA (1985) ^{1}H-NMR study of gramicidin A transmembrane ion channel: head-to-head right handed single stranded helices. FEBS Lett 186:168–174

Berendsen HJC, van der Spoel D, van Drunen R (1995) GROMACS: A message-passing parallel molecular dynamics implementation. Comput Phys Commun 91:43–56

Bernéche S, Roux B (2003) A microscopic view of ion conduction through the K+ channel. Proc Natl Acad Sci USA 100:8644–8648

Busath DD, Thulin CD, Hendershot RW, Phillips LR, Maughan P, Cole CD, Bingham NC, Morrison S, Baird LC, Hendershot RJ, Cotten M, Cross TA (1998) Noncontact dipole effects on channel permeation. I. Experiments with (5F-Indole)Trp13 gramicidin A channels. Biophys J 75:2830–2844

Chang G, Spencer RH, Lee AT, Barclay MT, Rees DC (1998) Structure of the MscL homolog from mycobacterium tuberculosis: A gated mechanosensitive ion channel. Science 282:2220–2226

Chiu SW, Jakobsson E (1989) Stochastic theory of singly occupied ion channels. II. Effects of access resistance and potential gradients extending into the bath. Biophys J 55:147–157

Chung SH, Hoyles M, Allen TW, Kuyucak S (1998) Study of ionic currents across a model membrane channel using Brownian dynamics. Biophys J 75:793–809

Chung SH, Allen TW, Hoyles M, Kuyucak S (1999) Permeation of ions across the potassium channel: Brownian dynamics studies. Biophys J 77:2517–2533

Chung SH, Allen TW, Kuyucak S (2002) Conducting-state properties of the KcsA potassium channel from molecular and Brownian dynamics simulations. Biophys J 82:628–645

Cooper KE, Jakobsson E, Wolynes P (1985) The theory of ion transport through membrane channels. Prog Biophys Mol Biol 46:51–96

Corry B, Kuyucak S, Chung SH (2000) Tests of continuum theories as models of ion channels: II. Poisson-Nernst-Planck theory versus Brownian dynamics. Biophys J 78:2364–2381

Corry B, Hoyles M, Allen TW, Walker M, Kuyucak S, Chung SH (2002) Reservoir boundaries in brownian dynamics simulations of ion channels. Biophys J 82: 1975–1984

Corry B, Kuyucak S, Chung SH (2003) Dielectric self-energy in Poisson-Boltzmann and Poisson-Nernst-Planck models of ion channels. Biophys J 84:3594–3606

Dorman VL, Jordan PC (2004) Ion permeation free energy in gramicidin: A semi-microscopic perspective. Biophys J 86:3529–3541

Doyle DA, Cabral JM, Pfuetzner RA, Kuo A, Gulbis JM, Cohen SL, Chait BT, MacKinnon R (1998) The structure of the potassium channel: molecular basis of K^+ conduction and selectivity. Science 280:69–77

Dutzler R, Campbell EB, Cadene M, Cahit BT, MacKinnon R (2002) X-ray structure of a ClC chloride channel at 3.0 Å reveals the molecular basis of anion selectivity. Nature 415:287–294

Edwards S, Corry B, Kuyucak S, Chung SH (2002) Continuum electrostatics fails to describe ion permeation in the gramicidin channel. Biophys J 83:1348–1360

Eisenberg RS (1999) From structure to function in open ionic channels. J Membrane Biol 171:1–24

Elber R, Chen DP, Rojewska D, Eisenberg R (1995) Sodium in gramicidin: and example of a permion. Biophys J 68:906–924

Feig M, Brooks CL (2004) Recent advances in the development and application of implicit solvent models in biomolecule simulations. Curr Opin Struct Biol 14:217–224

van Gunsteren WF, Berendsen HJC (1982) Algorithms for Brownian dynamics. Mol Phys 45:637–647

Im W, Roux B (2002) Ion permeation and selectivity of OmpF Porin: a theoretical study based on molecular dynamics, Brownian dynamics, and continuum electrodiffusion theory. J Mol Biol 322:851–869

Jordan PC (1990) Ion–water and ion–polypeptide correlations in a gramicidin-like channel. Biophys J 58:1133–1156

Ketchem RR, Hu W, Cross TA (1993) High-resolution conformation of gramicidin A in a lipid bilayer by solid-state NMR. Science 261:1457–1460

Ketchem RR, Roux B, Cross TA (1997) High-resolution polypeptide structure in a lamellar phase lipid environment from solid state NMR derived orientational constraints. Structure 5:1655–1669

Koeppe RE, Killian JA, Greathouse DV (1994) Orientations of the tryptophan 9 and 11 side chains of the gramicidin channel based on deuterium nuclear magnetic resonance spectroscopy. Biophys J 66:14–24

Koumanov A, Zachariae U, Englehardt H, Karshikoff A (2003) Improved 3D continuum calculations of ion flux through membrane channels. Eur Biophys J 32: 689–702

Kuyucak S, Andersen OS, Chung SH (2001) Models of permeation in ion channels. Rep Prog Phys 64:1427–1472

Levitt DG (1986) Interpretation of biological ion channel flux data – Reaction-rate versus continuum theory. Ann Rev Biophys Biophys Chem 15:29–57

Li AJ, Nussinov R (1998) A set of van der Waals and Coulombic radii of protein atoms for molecular and solvent-accessible surface calculation, packing evaluation, and docking. Proteins 32:111–127

Li SC, Hoyles M, Kuyucak S, Chung SH (1998) Brownian dynamics study of ion transport in the vestibule of membrane channels. Biophys J 74:37–47

Lindahl E, Hess B, van der Spoel D (2001) GROMACS 3.0: a package for molecular simulation and trajectory analysis. J Mol Model 7:306–317

MacKerell AD Jr, Bashford D, Bellot M, Dunbrack RL Jr, Evanseck JD, Field MJ, Fisher S, Gao J, Guo H, Ha S, Joseph-McCarthy D, Kuchnir L, Kuczera K, Lau FTK, Mattos C, Michnick S, Ngo T, Nguyen DT, Prodhom B, Reiher WE III, Roux B, Schlenkrich M, Smith JC, Stote R, Straub J, Watanabe M, Wiorkiewicz-Kuczera J, Yin D, Karplus M (1998) All-atom empirical potential for molecular modeling and dynamics studies of proteins. J Phys Chem B 102:3586–3616

Mamonov AB, Coalson RD, Nitzan A, Kurnikova MG (2003) The role of the dielectric boundary in narrow biological channels: a novel composite approach to modeling single-channel currents. Biophys J 84:3646–3661

McGill P, Schumaker MF (1996) Boundary conditions for single-ion diffusion. Biophys J 71:1723–1742

Moy G, Corry B, Kuyucak S, Chung SH (2000) Tests of continuum theories as models of ion channels: I. Poisson-Boltzmann theory versus Brownian dynamics. Biophys J 78:2349–2363

Nadler B, Hollerbach U, Eisenberg RS (2003) Dielectric boundary force and its crucial role in gramicidin. Phys Rev E 68:021905

Partenskii MB, Jordan PC (1992) Theoretical perspectives on ion-channel electrostatics: continuum and microscopic approaches. Q Rev Biophys 25:477–510

Roux B, Karplus M (1993) Ion transport in the gramicidin channel: free energy of the solvated right-handed dimer in a model membrane. J Am Chem Soc 115:3250–3262

Roux B, Karplus M (1994) Molecular dynamics simulations of the gramicidin channel. Annu Rev Biophys Biomol Struct 23:731–761

Separovic F, Barker S, Delahunty M, Smith R (1999) NMR structure of C-terminally tagged gramicidin channels. Biochim Biophys Acta 67:48–56

Smith GR, Sansom MSP (1999) Effective diffusion coefficients of K^+ and Cl^- ions in ion channel models. Biophys Chem 79:129–151

Tian F, Cross TA (1999) Cation transport: an example of stuctural based selectivity. J Mol Biol 285:1993–2003

Townsley LE, Tucker WA, Sham S, Hinton JF (2001) Structures of gramicidins A, B, and C Incorporated into sodium dodecyl sulfate micelles. Biochemistry 40:11676–11686

Urry DW (1971) The gramicidin A transmembrane channel: a proposed π_{LD} helix. Proc Natl Acad Sci USA 68:672–676